The Role of the Electric Field in Triboelectric Charging of Two Component Xerographic Developers

E. J. Gutman and G. C. Hartmann
Joseph C. Wilson Center for Technology, Xerox Corporation, Webster, New York

Abstract

The role of the electric field at the toner–carrier interface must be considered to understand the triboelectric charging mechanisms of two-component xerographic developers. The interfacial electric field is the result of the charge exchanged during repeated contacts between toner particles and carrier beads. We present a refinement of our previous model for the interfacial electric field; the new model includes multiple layers of toner on a carrier bead and treats the surface charge distribution on each toner particle as discrete, rather than continuous. We find good agreement of the refined model with the measured dependence of toner charge-to-mass ratio on toner concentration. Finally, we discuss the relation between the single fittable parameter, A_o, and the characteristic energy levels of the component materials.

Introduction

Recently Anderson[1] presented a discussion of a surface-state model of triboelectric charging of two-component electrophotographic developers and compared model predictions to available experimental measurements, including those of Schein[2] and the present authors.[3] Anderson's form of the surface-state model predicts a linear relationship between the inverse of the toner charge-to-mass ratio *(q/m)* and the toner concentration. His predicted ratio of the slope to intercept depends on the surface density of states of toner and carrier, but becomes independent of the surface density of states in the high-density limit. Anderson's review of available experiments suggests that the high-density limit for the slope-to-intercept ratio agrees with the data to within about a factor of 4, but that the estimated magnitude of *q/m* differs from experiment by about two orders of magnitude.

In our earlier publication,[3] in addition to the data referenced above, we described a physical model for *q/m* that incorporated a microscopic surface-state model for electric field-dependent contact electrification, combined with a model that traced how the carrier bead and toner particle charge changed with developer agitation.

The electric field in the gap at the region of a particular contact, which we call E_g, is the sum of the fields due to the contact charge density exchanged during this contact plus the "external field" from charges outside the region of contact. This "external field," which we call the toner–carrier interfacial electric field, is from charges exchanged in previous contacts distributed on the carrier bead, toner particle, and neighboring toner particles. Our *q/m* model treats the effect of having a number of different materials on the surfaces of both toner and carrier. Schein[2] has also emphasized the importance of E_g in understanding *q/m*. In this study, we refine the model of the toner-carrier interfacial electric field, examine how this modifies our physical model for *q/m*, and compare the predictions to experimental data. We also show that the magnitude of *q/m* agrees with the measured value if factors such as microscopic surface roughness and the contact probabilities of the component materials are considered.

Comparisons of our earlier physical model to measurements of the dependence of *q/m* on toner concentration, *C*, show that the value of the parameter C_o (the *C* axis intercept) predicted by the model is about a factor of two larger than the measured value. This is a large discrepancy and we were motivated to investigate the problem further. The parameter C_o depends on the value of the electric field at the toner-carrier interface. In our earlier work, three simplifying assumptions were made concerning the calculation of the local electrostatic field:

1. The influence of neighboring carrier beads on the toner-carrier interfacial electric field was not addressed.
2. The effect on the toner–carrier interfacial electric field due to multiple layers of toner particles on the carrier bead was neglected. Consequently, the model was limited to a toner monolayer, whereas most practical systems involve multilayers.
3. The charge on each toner particle was assumed to be continuously distributed on the surface and, as a consequence, was represented as a point charge located at the center of the toner particle. In reality, the charge on each toner particle is distributed discretely, and possibly nonuniformly, over the toner particle surface.

The first four sections of this study investigate each of these effects. The remaining three sections present a modified model for *q/m* and compare the modified model with experimental measurements.

Influence of Neighboring Carrier Beads on the Interfacial Electric Field

The influence of neighboring carrier beads surrounding a carrier bead of radius *R* on the toner-carrier interfacial elec-

tric field was investigated, using a model for the electrostatic field in which a charged toner particle of radius r_0 is embedded in a spherical cavity between R and $R + 2r_0$. The surrounding carrier beads are represented by a region having uniform dielectric constant, starting at radius $R + 2r_0$ and extending to infinity. The normal electric field at the surface of the carrier bead represented by the inner dielectric sphere is

$$E = -\partial\phi\partial r\Big|_{r=R}, \tag{1a}$$

where ϕ is the potential in the cavity generated by the charged toner particle. It is convenient to measure the field in units of $q/4\pi\in_o r_o^2$, where q is the charge on the toner particle. From Eq. 1a, we define a dimensionless function $f(u)$ related to the normal field at the surface of the carrier bead to be,

$$f(u) = (4\pi\in_o r_o^2 / q)\partial\phi / \partial r\Big|_{r=R}, \tag{1b}$$

where $u = \cos\theta$. The magnitude of the field at the point of contact of the toner particle with the carrier bead is given by $f(1)$. An expression for $f(1)$ is derived in Appendix A for the geometry described above, and numerically calculated values of $f(1)$ are given in Table I. These results show that the effect of neighboring carrier beads is to reduce the interfacial field slightly, but the effect is less than 10% and is, therefore, small. This finding provides our rationale for neglecting this effect in the refined model for the toner–carrier interfacial electric field.

Table I. Influence of Neighboring Carrier Beads on the Strength of the Interfacial Electric Field between a Uniformly Charged Toner Particle of Radius r_o and a Spherical Dielectric Carrier Bead of Radius R*

$\in_1$	R/r_o	Electric field strength, $f(1)$, when $\in_3 = 1$	Electric field strength, $f(1)$, when $\in_3 = \in_1$
4	3	1.71	1.58
	10	1.64	1.54
	20	1.62	1.52
10	3	2.00	1.81
	10	1.88	1.73
	20	1.85	1.71

• The neighboring dielectric carrier beads are represented by a dielectric region surrounding a cavity of radius $R + 2r_0$ and extending to infinity. The dielectric constants of the carrier bead, cavity, and surrounding region are $\in_1$, $\in_2 = 1$, and $\in_3$, respectively.

Multiple Layers of Toner Particles on the Carrier Bead

We now develop a model for the contribution of the fields from all the toner particles surrounding the carrier bead to the toner-carrier interfacial electric field of the toner particle under study, which we take to be the one at the pole. Figure 1 illustrates the model geometry. The toner particles in the layer closest to the carrier surface are represented by a spherical shell of charge located at $R + r_0$, but open at the pole to accommodate the particle under study. The toner particles in the second layer are represented by a second shell of charge also open at the pole.

The radial position of the second layer of charge depends on how the toner particles pack on the carrier bead surface. Simple cubic stacking results in a location of $R + 3r_0$; however, particles in the second layer can be staggered relative to the first layer, resulting in a location $R+(1 + 3^{1/2})r_0$. We find that the numerical results are not very sensitive to this assumption. The first layer can accommodate at most $n_{mono} = 4p_f R^2/r_0^2$ particles, where p_f is the packing factor, of order 0.5 to 0.6. The remaining $n - n_{mono} - n_2$ particles go into the second layer. Once the second layer is filled, in principle a third layer could be populated.

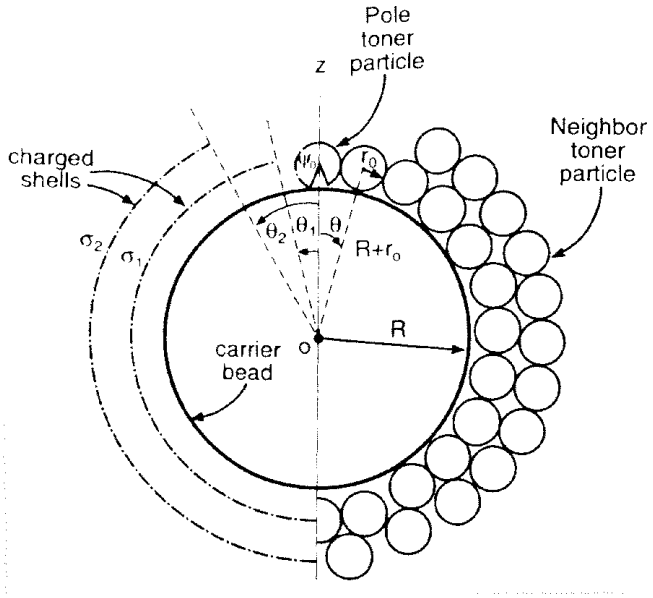

Figure 1. Geometry of the physical model. The right-hand side shows the assumed locations of toner particles; the left-hand side represents the electrostatic model.

We treat the pole toner particle uniquely and exclude it from both of the charged shells. For the first shell, following the approach of Ref. 3, this is done by defining a region at the pole subtended by the angle θ_1 and requiring that the surface integral be equal to $n_1 - 1$ charges:

$$\int_{\theta_1}^{\pi} 2\pi\sigma_1 (R+r_0)^2 \sin\theta d\theta = (n_1 - 1)q \tag{2}$$

For the first layer, with $n_1 \le n_{mono}$, the equivalent surface charge density is

$$\sigma_1 = \frac{n_1 q}{4\pi(R+r_0)^2}. \tag{3}$$

The angular size of the region at the pole is determined by substituting Eq. 3 into Eq. 2. This provides a relationship between the size of the region and n_1:

$$\sin^2\left(\frac{\theta_1}{2}\right) = \frac{1}{n_1}. \tag{4}$$

We also exclude from the pole region the n_2 particles in the second layer and assume that the charge n_2q is uniformly distributed between angle θ_2 and π, so that

$$\int_{\theta_2}^{\pi} 2\pi\sigma_2 (R+3r_o)^2 \sin\theta d\theta = n_2 q, \tag{5}$$

which gives

$$\sigma_2 = \frac{n_2 q}{4\pi(R+3r_o)^2} \frac{1}{\cos^2(\theta_2/2)}. \tag{6}$$

In this case, the equivalent surface charge density depends weakly on the choice of the angle θ_2. We choose θ_2 to be the same as the angle θ_1 for a monolayer in the first layer, defined by $\sin^2(\theta_1/2) = 1/n_{mono}$.

The total interfacial electric field at the pole is the sum of three electric field contributions: first, the toner particle at the pole; second, the other toner particles represented by the two partial shells of charge surrounding the carrier bead; and third, the charge on the carrier bead. The result is

$$\begin{aligned} 4\pi\in_0 E = \frac{-q}{r_o^2} f_1(1) - \int_{\theta_1}^{\pi} \frac{2\pi\sigma_1 (R+r_o)^2}{r_o^2} f_1(u)\sin\theta d\theta \\ - \int_{\theta_2}^{\pi} \frac{2\pi\sigma_2 (R+3r_o)^2}{r_o^2} f_2(u)\sin\theta d\theta + \frac{Q}{R^2}, \end{aligned} \tag{7}$$

where $u = \cos\theta$. Noting that $du = -\sin\theta d\theta$, Eq. 7 can be written

$$4\pi\varepsilon_0 E = -\frac{q}{r_0^2} f_1(1)\left\{1 - G_1(n_1) - G_2(n_2)\right\} + \frac{Q}{R^2}, \tag{8}$$

where

$$G_1(n_1) = \frac{n_1}{2f_1(1)} \int_{\cos\theta_1}^{-1} f_1(u)du$$

$$G_2(n_2) = \frac{n_2}{2f_1(1)} \int_{\cos\theta_2}^{-1} f_2(u)du.$$

Equation 8 is similar to the previous model[3] but now has two terms. Here $f_1(1)$ is the dimensionless parameter related to the strength of the interfacial field at the pole due to the charge of the pole toner particle. The functions $f_1(u)$ and $f_2(u)$ are the strength of the interfacial field at the pole due to the charge in the shells that represent the remaining $(n_1 - 1)$ particles in the first layer and the n^2 particles in the second layer.

An asymptotic expression for the field can be obtained from Eq. 8. Mathematically, n can be allowed to approach infinity, in which case mathematically the shells of charge become continuous at the pole and, as one can verify from Gauss's law, no longer contribute to the field at the surface of the carrier bead. The term $1 - G_1(n) - G_2(n)$ in Eq. 8 tends to zero, and therefore $-4\pi\in_o r_o^2 E/q \simeq n r_o^2/R^2$, which corresponds to the field due only to the carrier bead charge.

Electric Field Near the Surface of a Particle with a Discrete Surface Charge Distribution

Next we investigate how the electric field near a toner particle depends on details of the surface charge distribution on its surface. Hays[4] has investigated a related problem regarding the effect of patchy surface charge distributions on the adhesion of toner particles, and he found that the electrostatic force of adhesion can be greatly increased, depending on the surface charge distribution and the size of the contact area. We are motivated to examine discrete or patchy distributions of the surface charge, because the physical model for *q/m* deals with the charging dynamics of initially uncharged toner particles. As the developer is agitated and collisions occur between toner and carrier, the charge on the toner particles gradually increases and the surface distribution becomes patchy. In the patchy regions, there can be a single charge or several charges. Even in the case of a toner particle with single charges in each patch distributed homogeneously over its surface, the size of the regions between charges is surprisingly large. For example, a toner particle with 5 μm radius charged to 20 μC/gm has about 6×10^4 charges, and if these are spaced uniformly on the surface, the angle subtended by two adjacent charges is about 0.4°. Hence, it is likely that uncharged regions of the surface of the toner particle will continue to contact the carrier bead. We will show that a region this size without charge at the point of contact has an appreciable effect in reducing the strength of the toner–carrier interfacial field. Of course, the tonercarrier interfacial electric field is correspondingly increased in regions adjacent to the discrete charges.

The effect of a patchy surface charge distribution on the interfacial electric field should be greatest if a region without charge is located at the point of contact between the toner particles and carrier beads. We model this situation by smearing the discrete charges into a continuous shell of charge everywhere except in a circular region centered at the point of contact, as shown in Fig. 2. This is a reasonable model because of the inverse square dependence of field on distance, combined with the fact that the discrete charges represented by the continuous shell are located far from the point of contact. The charge distribution is embedded in a medium with permittivity $\in_o$.

Isolated Toner Particle

First we examine the field near an isolated toner particle. The radial electric field at point z (outside the sphere) on an axis aligned through the circular cap without charge is

$$E = \int_{\psi_o}^{\pi} \frac{dq\cos\beta}{4\pi\in_o S^2}, \tag{9}$$

where

$$\begin{aligned} dq &= 2\pi\sigma r_0^2 \sin\psi d\psi \\ \sigma &= q/(2\pi r_0^2(1+\cos\psi)) \simeq q/4\pi r_0^2 \\ \sin\beta &= r_0\sin\psi/s \\ S &= (r_0^2 + z^2 - 2r_0 z\cos\psi)^{1/2} \end{aligned}$$

and q and r_0 are the charge and radius of the toner particle, respectively. Equation 9 yields

$$E = \frac{q}{4\pi\in_o} \frac{1}{4r_o z^2} \left\{ 2r_o + \frac{(z^2 - r_o^2)}{S} - S \right\}, \tag{10}$$

where

$$S = \{(z - r_0)^2 + 4r_0 z\sin^2(\psi_0/2)\}^{1/2}.$$

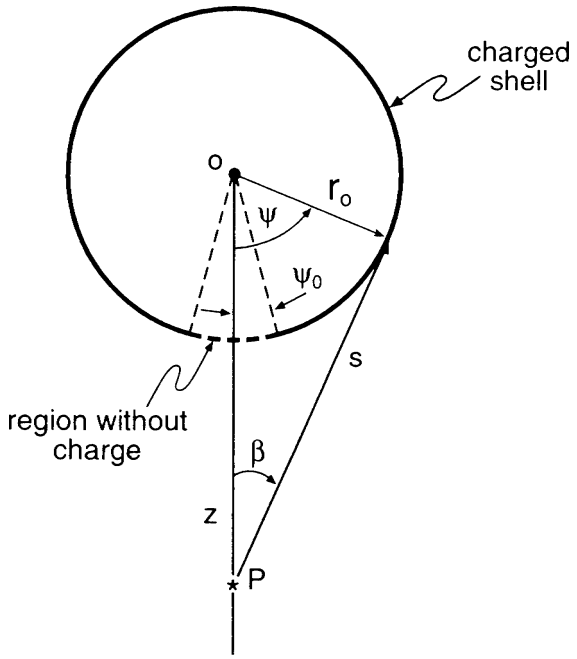

Figure 2. Geometry for the calculation of the electrostatic field outside a charged spherical shell having a region without charge on the z axis that subtends an angle ψ_o.

If the charge shell is assumed to be closed, that is, $\psi_o = 0$, then the field reduces to the expected result $E \rightarrow q/(4\pi\epsilon_o z^2)$. However, if ψ_o is small but nonzero, the strength of the field near the surface of the particle is considerably reduced. This is illustrated in Fig. 3, where Eq. 10 is plotted as a function of the distance from the surface of the particle. Table II shows how the field strength at the surface depends on the size of the region without charge. Both Fig. 3 and Table II show that very close to the surface, the field is approximately 50% of the case of a continuous, uniform distribution. Moreover, the value is only weakly influenced by the choice of ψ_o.

Toner Particle Adjacent to a Dielectric Sphere

Next we examine how this result is modified if the toner particle is near a dielectric sphere. The toner-carrier interfacial electric field for a spherical toner particle having a region without surface charge at the point of contact is examined in Appendix B. There, an analytic expression was found for a ring of charge near a dielectric sphere. Ideally, we would like to integrate this solution over the surface of the toner particle from ψ_o to π, by analogy to Eq. 9. However, this is cumbersome, and we have chosen instead to approximate the integral of the patchy surface distribution by summing the fields from a number of rings of appropriate diameter and position. Because of the weak dependence of the interfacial field on ψ_o outlined in the previous paragraph, as few as only three rings are sufficient to obtain reasonable results. Numerical values of the interfacial field strength $f_1(1)$ are given in Table III. The result is similar to that for the isolated charged toner particle, namely, that the interfacial field strength is reduced approximately 50% for the "patchy" surface charge distribution compared with the continuous case.

To summarize this section, if the field strength at the surface of a charged, isolated toner particle with a continuous surface charge distribution is one unit, then near a small region without charge the field is reduced to about 0.5 units. If a dielectric carrier bead is brought close to the toner particle, the interfacial field approximately doubles to about 2 units for the continuous surface charge distribution, and approximately doubles to about 1 unit for the "patchy" case.

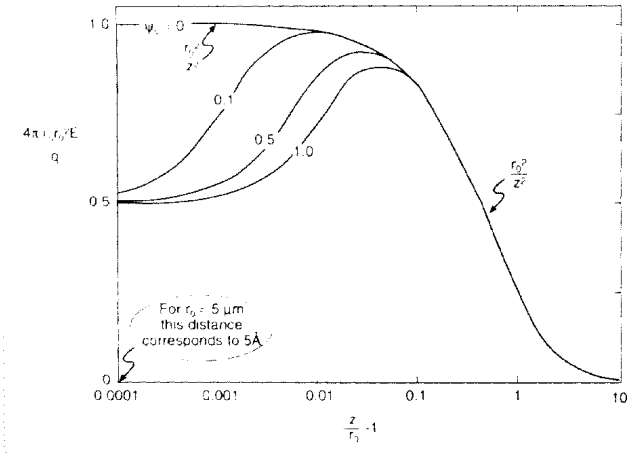

Figure 3. Calculated electrostatic field as a function of the distance z - r_o from the surface of a spherical shell of radius r_o. The shell has a small region without charge that subtends an angle ψ_o as shown in Fig. 2. The curve labeled $\psi_o = 0$ (no missing charge) is the function r_o^2/z^2. The surface of the sphere is located at $z = r_o$. As an example, if $z/r_o = 1.0001$ and $r_o = 5$ μm, then the distance from the surface is 5 Å.

Table II. Strength of the Electric Field at the Surface of an Isolated Toner Particle with Charge *q* and Radius r_o*

ψ_0	Surface area fraction of the region without charge	Field strength at the surface
0	none	1.0
0.1°	8×10^{-7}	0.53
0.5°	2×10^{-5}	0.50
1.0°	8×10^{-5}	0.50

* The toner particle has a region with no charge that subtends an angle y_o.

Table III. Strength of the Interfacial Electric Field $f_1(1)$ between a Toner Particle Having Charge *q* and Radius r_o, in Contact with a Dielectric Carrier Bead Having Dielectric Constant 10*

R/r_o	$f_1(1)$ for a uniform surface charge distribution	$f_1(1)$ for a "patchy" surface charge distribution represented by 3 rings of charge
3	2.00	1.05
10	1.88	0.94
20	1.85	0.91

* The two columns compare the field strength for uniform and "patchy" distributions of surface charge on the toner particle.

When the surface charge distribution on each toner particle includes a small region without charge at the point of contact, Eq. 7 for the total interfacial field strength is unchanged. The value of $f_1(l)$ is reduced approximately 50%, as discussed above and shown in Table III. The values for the integrals due to the other toner particles are unchanged because the functions $f_1(u)$ and $f_2(u)$ are not modified by the region without charge on the toner surface except when $u \simeq 1$ very near the pole of the carrier.

Dependence of Interfacial Electric Field on Toner Surface Charge Distribution and Number of Toner Particles

We now return to Eq. 8, which predicts how the toner–carrier interfacial electric field depends on the number of toner particles. Results of numerical calculations of Eq. 8 are shown in Fig. 4. Curve a is for the case where each toner particle has a continuous surface charge distribution, and it represents the extension of the electrostatic model of Ref. 3 to multiple layers. In this case, the function $f_1(u)$ is Eq. 19 of Ref. 3; the function $f_2(u)$ is similar, but the distance to the second charged shell is appropriately adjusted. Curves b and c show the effects of assumptions about discrete toner surface charge distributions. Curve b is for toner particles where the surface charge distribution is represented by 3 rings of charge. Complete expressions for $f_i(u)$ were used in the numerical calculation; Appendix B shows explicit expressions for $f_1(1)$ only. Curve c is for toner particles having a cap-shaped region without charge at the point of contact. In this case, the value of $f_1(l)$ is 50% of the value used to calculate Curve a, whereas for $u \neq 1$ the values of the functions $f_i(u)$ are the same as those used in Curve a.

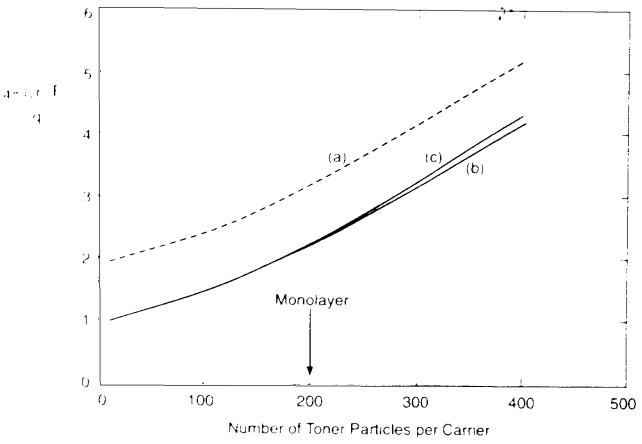

Figure 4. Dependence of the calculated toner-carrier interfacial electrostatic field on the number n of toner particles for the multilayer model, Eq. 8. The field is in units $q/4\pi\epsilon r_o^2$. The carrier dielectric constant is 8 and the ratio R/r_0 is 10. Curve a is for toner particles having a continuous surface charge distribution. Curve b is for toner particles where the toner surface charge distribution is represented by 3 rings of charge. Curve c is for toner particles having a small region without charge at the point of contact.

From Fig. 4, we note that the value of the interfacial electric field for the continuous toner surface charge distribution is quite different from the discrete cases. Second, the value of the intercept with the abscissa is different by about a factor of two. Third, the results for the two discrete surface charge distributions are essentially equivalent despite the fact that the details of the surface charge distributions are quite different. This is because of the inverse square dependence of field on distance.

Modified Model for q/m

The modified expression Eq. 8 for the toner-carrier interfacial electric field can now be substituted into the physical model for *q/m*. We find

$$q/m = \frac{A_o}{C + \Omega_o(C)}\left[1 - \exp(-t/\tau)\right], \qquad (11)$$

and for $n < n_{mono}$

$$\Omega_0(C) = \frac{r_0\rho_t}{R\rho_c} f_1\left\{1 - G_1(n)\right\}$$

and for $n > n_{mono}$

$$\Omega_0(C) = \frac{r_0\rho_t}{R\rho_c} f_1\left\{1 - G_1(n_{mono}) - G_2(n - n_{mono})\right\}$$

and where n and C are related by $n = CM/m$, and m and M are the toner and carrier masses, respectively. For long mixing times, a simplified expression for m/q can be obtained from Eq. 11 to compare with experimental values:

$$m/q = \frac{1}{A_o}\left[C + \Omega_o(C)\right] \qquad (12)$$

Comparison of Physical Model with Experiment

The physical model for *q/m*, Eq. 11, was compared with experimental results by fitting the model to measurements of m/q plotted versus toner concentration C with one adjustable parameter, A_o.

Figure 5 compares the model and experiment for toner and carrier materials having $R/r_o = 10$ and materials composition described by Nash.[5] The carrier is an uncoated nickel ferrite bead with mass density 5.0 g/cc and diameter equal to 100 μm. The dielectric constant of the ferrite carrier material was taken[6] to be 8, consistent with values in the literature for the polarization of bound charge carriers; it seems reasonable to assume that there are no free charge carriers in the bulk of the carrier bead. The toner comprises a copolymer of polystyrene and *n*-butylmethacrylate, melt-mixed with 10% loading of a furnace carbon black. The toner packing factor p_f is estimated to be 0.55. Figure 5 shows parametric fits of the physical model with A_o as the only adjustable variable, calculated using both continuous and discrete toner surface charge distributions. Using the measured values for the parameters in the expression for $\Omega_o(C)$ in Eq. 11, the discrete surface charge distribution model gives a good fit, much better than the continuous model. It is not possible to make the continuous model match the data set for any choice of the fittable parameter A_o. This observation provides further support for the discrete surface charge distribution model.

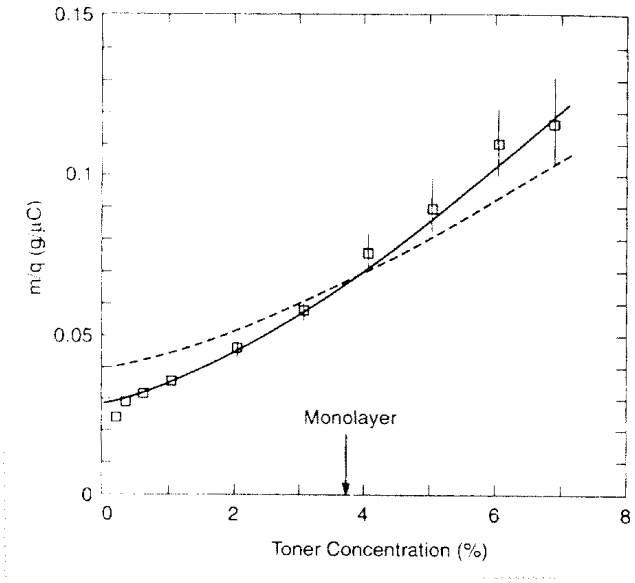

Figure 5. Comparison of the physical model with experimental measurements of toner q/m for materials having R/r_0 = 10. The physical model has one adjustable parameter, A_o; the fitted value is 0.63 μC/g. The solid curve *is calculated assuming a discrete toner surface charge distribution. The* dashed curve *is calculated for a continuous toner surface charge distribution; it is not possible to match the data set for any choice of the fittable parameter A_o. A monolayer toner coverage is indicated by the* vertical arrow. *The* bars *on the data represent an estimate of the measurement precision of about 1 μC/gm.*

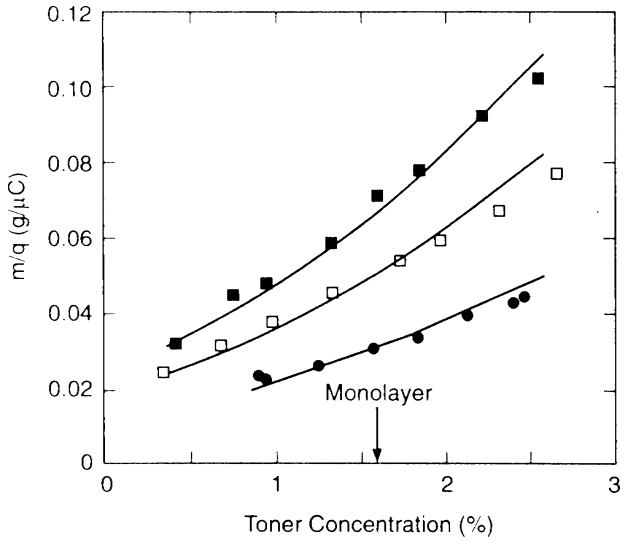

Figure 6. Comparison of the physical model with experimental measurements made by Schein[2] of toner q/m for materials having R/r_o = 20. Measurements are shown for three toners having different concentrations of charge control additive. A monolayer toner coverage is indicated by the vertical arrow.

Figure 6 compares measurements by Schein[2] for three toners, each having different concentrations of a charge control additive (CCA). The carrier consists of 200 μm diameter steel beads; the ratio of carrier bead to toner particle size is R/r_o = 20. The dielectric constant of the steel carrier bead is assumed to be > 50, and the mass density is 7.7 g/cc. The toner packing factor is estimated to be 0.6. Figure 6 shows parametric fits of the discrete toner surface charge model, with A_o as the only adjustable variable. Measured values were used for the parameters in the expression $\Omega_o(C)$. The fitted values of A_o are plotted versus the CCA concentration in Figure 7, which suggests that A_o increases monotonically with CCA concentration.

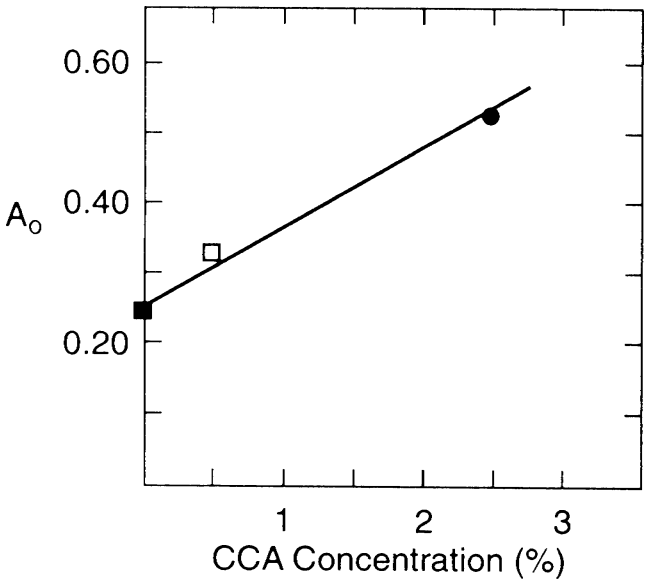

Figure 7. Dependence of the parameter A_o on charge control additive concentration. Values are taken from the fitted curves shown in Fig. 6.

Finally, we compare our model with experiment for materials for which R/r_0 = 5.3. Figure 8 compares the data and the model prediction with A_o the only adjustable parameter; its value is 0.58 μC/g. The carrier is a polymer-coated iron bead with diameter equal to 70 μm, and with mass density 7.7 g/cc. The dielectric constant was assumed to be >50. The toner particles were styrene-butadiene resin melt-mixed with a pigment.

Table IV. Parameters Resulting from Least Squares Fits of a Straight Line to the Experimental Data from Fig. 5 and to the Predictions of the Discrete Toner Surface Charge Model Evaluated at the Same Toner Concentrations

Parameter	Straight line fit to data	Straight line fit to model
Coefficient of determination, R^2	0.992	0.987
Y intercept (g/μC)	0.0231	0.0217
Slope (g/μC)	1.377 ± 0.044	1.341 ± 0.055

The refined model predicts a slightly nonlinear dependence of m/q on toner concentration that agrees with measurements. However, we believe it is very difficult to discriminate between a straight-line fit to the data and the

refined model, which has a small amount of curvature. For example, a linear least squares fit to the data in Fig. 5 gives a very good result; likewise, a linear least squares fit to the pseudodata set consisting of the model predictions at corresponding toner concentrations also gives a good fit; see Table IV. Therefore it is difficult to test the model on the basis of curvature alone.

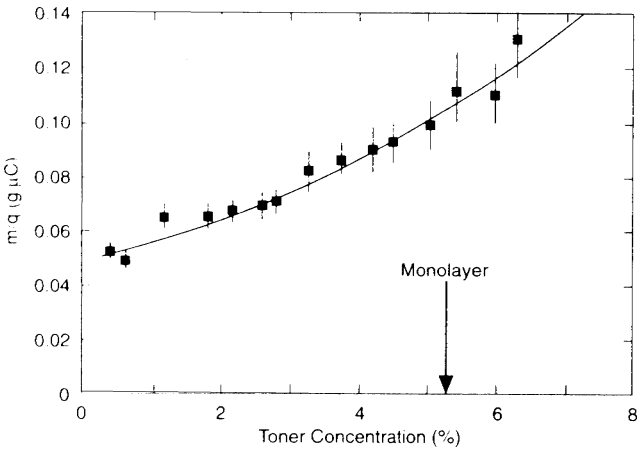

Figure 8. Comparison of the physical model with experimental measurements of toner q/m for materials having $R/r_o = 5.3$. The physical model has one adjustable parameter, A_o; the fitted value is 0.58 μC/g. A monolayer toner coverage is indicated by the vertical arrow. *The* bars *on the data represent an estimate of the measurement precision of about 1 μC/gm.*

Discussion

A standard assumption of previous investigations of toner *q/m* is that the electric field near a toner particle can be modeled by assuming a uniform, continuous toner surface charge distribution. The assumption of a uniform continuous distribution is, of course, electrostatically equivalent to assuming that all the charge is located at the center of the toner particle. However, we have shown that for discrete charges distributed on the surface, rather than a continuous distribution, the field very close to or adjacent to the surface is reduced by about 50% in the areas between the charges. We have characterized the charge-free areas by the subtended angle and have shown that the interfacial field is reduced 50%, even if the angle is as small as 0.01°, so that the effect most certainly occurs for fully charged toner particles, for which the angle is of order 0.4°.

The electric field part of the physical model was extended to include multiple toner layers on the carrier bead. This was done by considering the dependence of the interfacial electric field on the charges of the toner particles in the second layer. This enabled a straightforward extension of the physical model to toner concentrations exceeding the value corresponding to a monolayer. The effect of neighboring carrier beads was briefly considered and found to be small compared with the other considerations.

The physical model with the improved interfacial electric field was fitted to measurements of the dependence of m/q on toner concentration with only one adjustable parameter, A_o. The model provides a framework that links A_o to the microscopic parameters of the component materials. From the physical model,[3]

$$A_o = \frac{a}{s}\frac{4\pi R^2}{M}\frac{\epsilon_o}{ed}\left\{\sum_j^{TS} P_j\mu_j - \sum_i^{CS} P_i\mu_i\right\}, \qquad (13)$$

where $M = 4\pi\rho_c R^3/3$ is the carrier mass, a is the microscopic area of contact of asperities between toner and carrier beads, s is the area of localized conductivity on the surface of the toner particle, e is the electronic charge, d is the electronic tunneling length, P_j and P_i are contact probabilities, μ_j and μ_i are the characteristic energy levels of each of the component materials present on the surfaces of the toner and carrier beads, and *TS* and *CS* refer to sums over the toner and carrier component materials, respectively.

Using the measured value $A_o = -0.63$ μC/g determined from Fig. 5, and assuming $d = 10$ Å, we find $(a/s)(\sum P_j\mu_j - \sum P_i\mu_i)/e = -5.6$ mV. We now briefly examine if this value is consistent with estimates of the characteristic energies and contact probabilities of the component materials, and with estimates of microscopic surface roughness related to the value of *a/s*.

In the framework of the physical model, the parameter s is bounded by two values. The smallest value is equal to the microscopic area of contact of the asperities, that is, $s = a$. The largest value for s is the projected geometric area of contact. Therefore, the ratio *a/s* is related to the microscopic surface roughness and contact pressure, although we have not examined this relationship in detail.

The importance of microscopic surface roughness and the relation to contact charging has been emphasized by Coste and Pechery.[7] They measured the dependence of the actual contact area on surface roughness. Using their data and our estimate that the combined roughness of carrier and toner surfaces is about 0.5 to 1 μm, we estimate the ratio of actual to projected geometric contact area to be about 0.2 for our materials. Coste and Pechery also found that the relationship between surface charge density and contact area is, in general, nonlinear; however, it is approximately linear for values of roughness similar to that of our materials.

For an uncoated carrier and a toner comprising resin and carbon black, the term $(\sum P_j\mu_j - \sum P_i\mu_i)/e$ can be expressed as $P_f\mu_f - \{P_{cb}\mu_{cb} + (1 - P_{cb})\mu_r\}$, where the subscripts *f*, *cb,* and *r* refer to the carrier ferrite, toner carbon black, and toner resin, respectively. Because the carrier is uncoated, $P_f = 1.0$. The carbon black concentration in our toner is 10%; therefore $P_{cb} \simeq 0.1$.

Julien[8] reports values of $\mu_r = -4.1$ eV for polymethylmethacrylate and $\mu_{cb} = -4.8$ eV for oxidized carbon black. We have not found a published value for the work function of ferrite, which is a polycrystalline material comprising the elements nickel, iron, and oxygen. We have made an estimate of the ferrite work function, assuming that it is the average of the work functions deduced from Kelvin potential measurements of metallic surfaces in vacuum and air—and presuming that the latter measurements include metal oxides. Harper[9] reports values for the work functions of nickel and steel relative to gold of 0.35 and 0.45 eV, respectively, and Davies[10] reports a value for gold of –4.6 eV. Consequently, we infer that the ferrite work function is $\mu_f \approx$

–4.2 eV; we emphasize that this is an extrapolation from the published experimental results.

Combining these estimates, we find $(a/s)(\sum P_j\mu_j - \sum P_i\mu_i)/e \simeq -6$ mV, which is close to the measured value of –5.6 mV. We conclude that reasonable agreement between the measured and modeled values of A_o is obtained if one includes the effects of the characteristic energies and contact probabilities of the toner and carrier component materials and the effects of microscopic surface roughness in the region of contact.

In summary, a refined physical model of *q/m* was based on investigation of the toner–carrier interfacial electric field and its dependence on three contributions; multiple layers of toner particles on the carrier bead, details of the toner surface charge distribution, and the surrounding carrier beads. The effect of the surrounding carrier beads was found to be small and was therefore neglected. The investigation of multiple layers of toner on the carrier bead resulted in a straightforward extension of the model. The discrete nature of the toner surface charge distribution was found to be important; in particular, the toner–carrier interfacial electric field must be calculated using a discrete toner surface charge distribution rather than a continuous one. The continuous assumption overestimates the interfacial field strength by almost a factor of two, whereas the discrete case provides an accurate value and correctly predicts the dependence of *m/q* on toner concentration. Finally, we have shown that there is reasonable numerical agreement between the measured value of A_o and the value predicted by the physical model that uses the characteristic energies and fractional area coverages of the component materials.

Acknowledgments

We are grateful to L. B. Schein for providing to us tables of his xerographic measurements from Ref. 2 for comparison to the model, and to R. J. Nash for several helpful discussions. We thank C. D. Zimmer and R. J. Hodgson for experimental measurements.

Appendix A: Point Charge Inside a Dielectric Cavity

This appendix summarizes a calculation of the electrostatic field of a point charge q located at radius $\xi = r_1 + r_o$ in a region defined by a spherical cavity in a dielectric material of radius r_3 that contains a dielectric sphere of radius r_1. The dielectric constant of the material is $\in_1$, and the dielectric constant of the cavity is $\in_2$. The geometry, shown in Fig. A1, is a model for a charged toner particle of radius r_o near a dielectric carrier bead that is surrounded by other dielectric carrier beads.

The potential in each region can be represented by

$$\begin{aligned}\phi_1 &= \sum_0^\infty a_n r^n P_n(\cos\theta)\\ \phi_2 &= q/(4\pi\in_2 r_2) + \sum_0^\infty (b_n r^n + c_n/r^n + 1)P_n(\cos\theta)\\ \phi_3 &= \sum_0^\infty d_n P_n(\cos\theta)/r^{n+1},\end{aligned} \tag{A1}$$

where $P_n(\cos\theta)$ is the Legendre polynomial of order n.

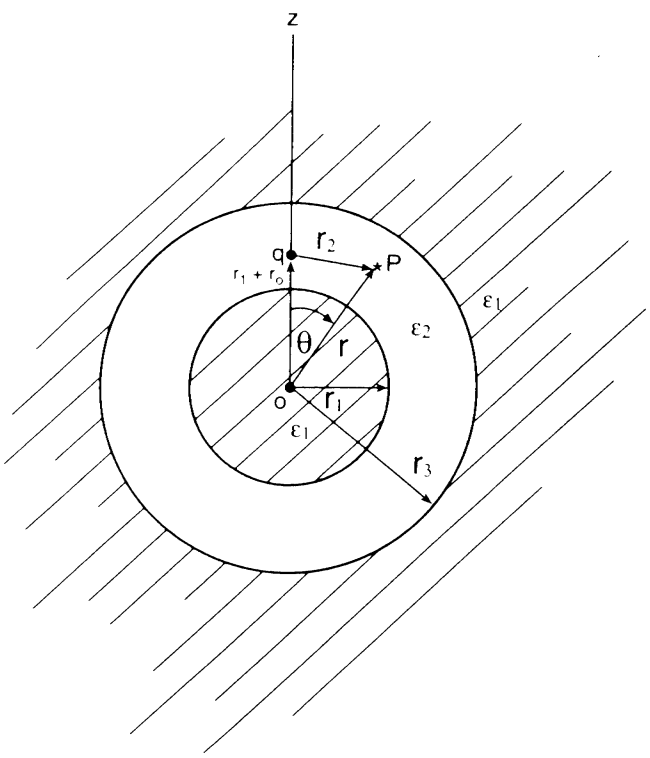

Figure A1. Geometry for calculation of the electrostatic field at point P of a charge q located at radius $\xi = r_1 + r_0$ in a three-dimensional space defined by a spherical cavity of radius r_3 that contains a dielectric sphere of radius r_1.

The boundary conditions are

$$\begin{aligned}&\text{at } r = r_1 && \phi_1(r_1) = \phi_2(r_1)\\ &&& \in_1 \partial\phi_1/\partial r\Big|_{r_1} - \in_2 \partial\phi_2/\partial r\Big|_{r_1} = 0\\ &\text{at } r = r_3 && \phi_2(r_3) = \phi_3(r_3)\\ &&& \in_2 \partial\phi_2/\partial r\Big|_{r_3} - \in_1 \partial\phi_3/\partial r\Big|_{r_3} = 0.\end{aligned} \tag{A2}$$

The term $1/r_2$ is expanded in Legendre polynomials according to

$$\begin{aligned}1/r_2 &= (1/\xi)\sum_0^\infty (r/\xi)^n P_n(\cos\theta) \quad \text{if } r < \xi\\ 1/r_2 &= \sum_0^\infty (\xi n/r^n + 1)P_n(\cos\theta) \quad \text{if } r > \xi.\end{aligned} \tag{A3}$$

The solution is obtained by straightforward substitution of Eqs. A1 and A3 into Eq. A2 and solving for the coefficients a_n, b_n, c_n, and d_n. We are particularly interested in the strength of the electric field at the point of contract of the toner particle to the dielectric carrier bean, at $r = r_1$. The value of the field there is

$$E = \partial\phi_2/\partial r\Big|_{r_1} \tag{A4}$$

It is convenient to define a dimensionless function $f(u)$ by the relation

$$f(u) = (4\pi \in_o r_o^{\,2} / q)\partial\phi_2 / \partial r \Big|_{r_1}, \qquad \text{(A5)}$$

where $u = \cos\theta$. This function is proportional to the normal field at the surface of the sphere. For this problem, we find

$$f(1) = \frac{r_o^{\,2}}{\xi^2}\sum_{n=0}(r_1/\xi)^{n-1} \qquad \text{(A6)}$$

$$+\frac{r_o^{\,2}}{\xi^2}\sum_{n=0}^{x}$$

$$\frac{n^2(n+1)(\rho-1)^2(r_1/r_3)^{2n+1}(r_1/\xi)^{n-1} - n(n+1)(\rho-1)(\rho n+n+1)(\xi/r_3)^{n+2}(r_1/r_3)^{n-1}}{(\rho n+n+1)\{n+\rho(n+1)\} - n(n+1)(\rho-1)^2(r_1/r_3)^{2n+1}}$$

$$-\frac{r_o^{\,2}}{\xi^2}\sum_{n=0}^{x}$$

$$\frac{n(n+1)^2(\rho-1)^2(\xi/r_3)^{n+2}(r_1/r_3)^{n-1} - n(n+1)(\rho-1)\{n+\rho(n+1)\}(r_1/\xi)^{n-1}}{(\rho n+n+1)\{n+\rho(n+1)\} - n(n+1)(\rho-1)^2(r_1/r_3)^{2n+1}}$$

and where $\rho = \in_1/\in_2$ and $\xi = r_1 + r_o$ as before.

This reduces to the expression for $f(1)$ given by Eq. B19 of Ref. 3 if $r_3 \to \infty$. Numerical values of $f(1)$ calculated from Eq. A6 are displayed in Table III in the main text. The summations were continued until the value was stable in the third decimal place; in some cases this required over 800 terms.

Appendix B: Ring of Charge Near a Dielectric Sphere Used to Approximate a "Patchy" Toner Charge Distribution

This appendix summarizes a calculation of the electrostatic field of a ring of charge q and radius b located in a dielectric medium with permittivity $\in_2$ at position $\xi = r_1 + a$ from a dielectric carrier bead of radius r_1 and dielectric constant $\in_1$. The geometry is shown in Fig. B1.

For a ring of charge in free space, the potential at an arbitrary point can be found in many texts. Smythe[11] gives the following result:

$$V_R = \frac{q}{4\pi\in_o}\frac{1}{c}\sum\left(\frac{r}{c}\right)^n P_n(\cos\alpha)P_n(\cos\theta)$$

$$r < c \text{ or } \theta \neq \alpha,\ r = c$$

$$V_R = \frac{q}{4\pi\in_o}\frac{1}{c}\sum\left(\frac{c}{r}\right)^{n+1} P_n(\cos\alpha)P_n(\cos\theta)$$

$$r > c \text{ or } \theta \neq \alpha,\ r = c$$

where c is the distance from the center of the sphere to a point on the ring and α is the angle between the z axis and the vector c. The potential of the ring of charge near a dielectric sphere can be found by writing the potential in Region I inside the dielectric sphere ($r < r_1$), and in Region II outside the dielectric sphere ($r > r_1$),

$$\begin{aligned}\Phi_{\mathrm{I}} &= \sum a_n r^n P_n(\cos\theta), \quad r < r_1\\ \Phi_{\mathrm{II}} &= \frac{q}{4\pi\in_o}\frac{1}{c}\sum\left(\frac{r}{c}\right)^n P_n(\cos\alpha)P_n(\cos\theta)\\ &\quad +\sum(b_n/r^{n+1})P_n(\cos\theta),\\ &\quad r_1 < r < c \text{ or } \theta \neq \alpha,\ r = c\end{aligned} \qquad \text{(B1)}$$

or

$$\begin{aligned}\Phi_{\mathrm{II}} &= \frac{q}{4\pi\in_o}\frac{1}{c}\sum\left(\frac{c}{r}\right)^{n+1} P_n(\cos\alpha)P_n(\cos\theta)\\ &\quad +\sum(b_n/r^{n+1})P_n(\cos\theta),\\ &\quad r_1 < c < r \text{ or } \theta \neq \alpha,\ r = c\end{aligned}$$

The boundary conditions at $r = r_1$ are

$$\begin{aligned}&\Phi_{\mathrm{I}}(r_1) = \Phi_{\mathrm{II}}(r_1)\\ &\in_1 \frac{\partial\Phi_{\mathrm{I}}}{\partial r}\Big|_{r=r_1} = \in_2 \frac{\partial\Phi_{\mathrm{II}}}{\partial r}\Big|_{r=r_1}.\end{aligned} \qquad \text{(B2)}$$

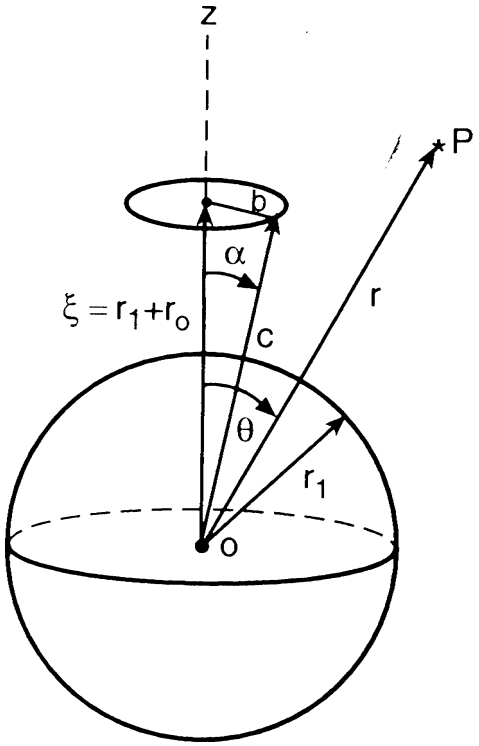

Figure B1. Geometry for calculation of the electrostatic field at point P *for a ring with charge* q *near a dielectric sphere with radius* r_1. *The ring has diameter* b *and is centered at* $\xi = r_1 + a$.

The solution is obtained by substitution of Eqs. B1 into Eqs. B2 and solving for the coefficients. We are particularly interested in the electric field strength on the surface of the dielectric carrier bead at the pole. The value of the field strength, $f(1)$, at the pole of the carrier bead for a ring of charge is

$$f(1)=\frac{4\pi\epsilon_0 {r_o}^2}{q}\sum_{n=0}^{\infty}\frac{q}{4\pi\epsilon_0}\frac{1}{c^2}\left(\frac{r_1}{c}\right)^{n-1} \bullet P_n(\cos\alpha)\frac{n(2n+1)\epsilon_1}{n\epsilon_1+(n+1)\epsilon_2}. \quad \text{(B3)}$$

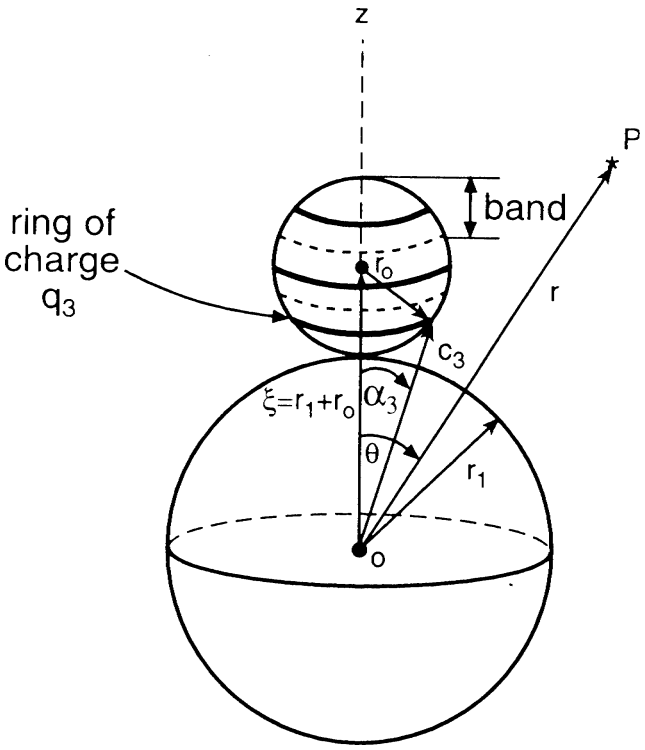

Figure B2. Geometry for calculation of the electrostatic field at point P of a nonuniform distribution of surface charge on a spherical toner particle near a dielectric carrier bead. The nonuniform toner surface charge distribution is represented in the illustration by three rings of charge.

A "patchy" surface charge distribution on a toner particle near a dielectric carrier bead can be approximated by summing the contributions from several charged rings. The amount of charge in each ring is proportional to the surface area of imaginary bands defined in such a way that the rings are centered in them. The total potential for the particle is the summation ofthe potentials due to each charged ring. The location of each ring is specified by the angle α_i and the distance c_i. The geometry is shown in Fig. B2. The strength of the electric field at the pole of the dielectric carrier bead is

$$f(1)=\frac{4\pi\epsilon_0 {r_o}^2}{q}\sum_{n=0}^{\infty}\frac{1}{4\pi\epsilon_0}\sum_{k=1}\frac{q_k}{{c_k}^2}\left(\frac{r_1}{c_k}\right)^{n-1} P_n(\cos\alpha_k)\frac{n(2n+1)\epsilon_1}{n\epsilon_1+(n+1)\epsilon_2}, \quad \text{(B4)}$$

where q_k is the charge in the k-th band and $\sum q_k = q$.

We found that three bands (0° to 60°, 60° to 120°, and 120° to 180°) with charged rings centered at 30°, 90°, and 150° and with 25, 50, and 25% of the charge, respectively, is a good approximation for a charged particle with a missing region of charge at the point of contact with the carrier bead. Numerical values of $f(1)$ using Eq. B4 are displayed in Table III.

Appendix C: Errata for Reference 3

Equations B12, B13, B15, and B21 contain errors. Using the notation of Ref. 3, the correct expressions are:

$$\lim_{\text{large } n} G(n)\rightarrow\frac{f'(1)}{nf(1)} \quad \text{(B12)}$$

$$\lim_{\text{large } n} 4\pi\epsilon_0 E\rightarrow\frac{Q}{R^2}\left[1+\frac{f'(1)}{f(1)^2}(r/R)^2(C_o/C)^2\right] \quad \text{(B13)}$$

$$f(x)=\frac{-(y_1-y_2x)r^2}{\left[({y_1}^2+{y_2}^2)-(2y_1y_2x)\right]^{3/2}}$$

$$+\frac{\frac{Rr^2}{y_2}\left(y_1-\frac{Rx^2}{y_2}\right)}{\left[{y_1}^2+\frac{R^4}{{y_2}^2}-\frac{2y_1R^2x}{y_2}\right]^{3/2}}-\frac{Rr^2}{y_2{y_1}^2} \quad \text{(B15)}$$

$$f(1)\gtrsim 1+\frac{\epsilon-1}{\epsilon+1}\left[1+\frac{r}{r+R}\right] \quad \text{(B21)}$$

The sentences immediately following Eq. B21 should be replaced by:

"Compared to Eq. B17, Eq. B21 is identical in the limit $\epsilon\rightarrow\infty$. Values of $f(1)$ can be found by numerically summing the series. We find values of 1.71, 2.00, and 2.25 for $R/r = 3$ and $\epsilon = 4$, 10, and ∞, respectively; and 1.64, 1.88, and 2.09 for $R/r = 10$ with corresponding values of ϵ. The approximate analytic expression above gives values within 1% of these values."

References

1. J. H. Anderson, A comparison of experimental data and model predictions for tribocharging of two-component electrophotographic developers, *J. Imaging Sci. Technol.* **38**: 378 (1994); (see page 189, this publication).
2. L. B. Schein, Theory of toner charging, *J. Imaging Sci.*

Technol. **37**: 1 (1993).
3. E. J. Gutman and G. C. Hartmann, Triboelectric properties of two-component developers for xerography, *J. Imaging Sci. Technol.* **36**: 335 (1992).
4. (a) D. A. Hays and W. H. Wayman, Adhesion of a nonuniformly charged dielectric sphere, *J. Imaging Sci.* **33**: 160 (1989); and (b) D. A. Hays, Toner adhesion, *Proceedings of the Seventeenth Annual Meeting and the Symposium on Particle Adhesion,* 1994, The Adhesion Society, Orlando, FL, Feb. 20-23, p. 91.
5. R. J. Nash, The effect of external toner additives on the conductivity of ferrite-base, xerographic developers, *Proceedings of SPSE-IS&T's 5th International Congress on Advances in Non-Impact Printing Technologies*, Nov. 12-17, 1989, San Diego, CA, p. 82.
6. P. A. Miles, W. B. Westphal, and A. von Hippel, Dielectric spectroscopy of ferromagnetic semiconductors, *Rev. Mod. Physics* **29:** 279 (1957).
7. J. Coste and P. Pechery, Influence of surface profile in polymer-metal contact charging, *J. Electrostatics* **10:** 129 (1981).
8. P. C. Julien, in *Carbon Black-Polymer Composites*, E. K. Sickel, Ed., Marcel Dekker Inc., New York, 1982, p. 189.
9. W. R. Harper, *Contact and Frictional Electrification*, Clarendon, Oxford University Press, New York, 1967.
10. D. K. Davis, *J. Phys. D*. **2:** 1533 (1969).
11. W. R. Smythe, *Static and Dynamic Electricity*, McGraw Hill Book Company, New York, 1950, p. 139.